JOURNAL OF SPACECRAFT AND ROCKETS
Vol. 31, No. 6, November–December 1994

Some Aspects of the Aerodynamics of Separating Strap-ons

K. K. Biswas* and C. G. Krishnan
Vikram Sarabhai Space Centre, Thruvananthapuram, 695022, India

An aerodynamic model for analyzing strap-on separation is proposed. This model comprises both interference aerodynamics and free-body aerodynamics. The interference aerodynamics is primarily due to the close proximity of core and strap-ons. The free-body aerodynamics is solely due to the body geometry of the strap-ons. Using this aerodynamic model, the dynamics of separating strap-ons has been simulated in a six-degree-of-freedom mode to determine if a collision occurs. This aerodynamic model is very handy for various off-design studies relating to separating strap-ons.

Nomenclature

C_A	= aerodynamic axial-force coefficient
C_S	= aerodynamic side-force coefficient
C_{ym}	= aerodynamic yawing moment coefficient
d	= distance, m
$\boldsymbol{F}_A$	= force due to aerodynamics, N
$\boldsymbol{F}_S$	= force due to separation system, N
$\boldsymbol{F}_T$	= force due to thrust, N
I	= inertia tensor, kg·m^2
$\boldsymbol{M}_A$	= moment due to aerodynamics, N·m
$\boldsymbol{M}_T$	= moment due to thrust, N·m
$\boldsymbol{M}_S$	= moment due to separation system, N·m
m	= mass, kg
$\boldsymbol{V}$	= velocity, m/s
t	= time, s
$\boldsymbol{W}$	= body angular rates, deg/s
(W_x, W_y, W_z)	= components of $\boldsymbol{W}$, deg/s
β	= sideslip angle, deg
(ϕ, θ, ψ)	= attitude angles, deg

Subscript

0	= initial value (corresponding to time = 0)

Superscripts

I	= interference aerodynamics
i	= ith body
F	= free-body aerodynamics

Introduction

DURING the flight of strap-on launch vehicles, the strap-on boosters are usually separated in the denser atmosphere. A knowledge of aerodynamic characteristics of separating strap-ons is essential for the design of separation mechanisms. The ejection mechanism of the separation system imparts lateral forces on the separating strap-ons. The aerodynamic forces and moments play the critical role in the separation process if it occurs in a region of high aerodynamic pressure.

The aerodynamic characteristics of separating strap-ons are not amenable to theoretical investigations. The flowfield around such a configuration is highly complex, being dominated by mutual interference of multiple bodies in close proximity. For such a complicated flowfield, wind-tunnel experiments are the prime sources of reliable data. Sundaramoorthy et al.[1] investigated the problem of aerodynamics of strap-on separation in two ways, using a grid technique and a semicaptive-trajectory technique. In both of these investigations, extensive wind-tunnel tests were made. The parallel stage separation of a reusable booster, as in the Space Shuttle configuration, has been investigated by Decker[2] and Decker and Joseph[3] using experimental aerodynamics.

In order to know the aerodynamics of separating strap-ons at large angle of incidence (up to 5 deg), a model has been developed using the preliminary experimental results. In this model, it is assumed that the complex aerodynamic field of a separating strap-on is composed of free-body and interference aerodynamics. The free-body aerodynamic field is solely due to the body geometry of the strap-on and is primarily dependent on the angle of incidence, since the Mach-number change during the strap-on separation is negligible. The interference aerodynamic field is due to the proximity of the core and strap-ons. This field depends strongly on the gap between core and strap-on.

Using this model, the strap-on separation has been analysed[4] for a typical strap-on vehicle with an initial angle of incidence of 4 deg. In order to build robustness into the design of separation systems, 25% more adverse aerodynamics is used. Collision-free separation of strap-ons was demonstrated.

Mathematical Modeling of Separation of Strap-ons: Coordinate Frame

All the coordinate frames (Fig. 1) used in the present investigations are right-handed frames. The B frame is the usual body frame, and the L frame is the local inertial frame of Ref. 5. The L frame is parallel to the body frame at the time of initiation of separation. This frame moves with a uniform velocity corresponding to the velocity of the vehicle at the time of initiation of separation. The distance between the separating bodies are computed in this coordinate frame. The transformation $(\mathrm{TR})_L^B$ from L frame to B frame is achieved by three successive rotations as shown in Fig. 1.

Development of Equations of Motion

The basic equations of motion are derived assuming the bodies are rigid. These equations of motions for bodies participating in the separation are given in their respective body coordinate frame as

$$m^i \frac{\mathrm{d}\boldsymbol{v}^i}{\mathrm{d}t} + \boldsymbol{W}^i \times \boldsymbol{V}^i = \boldsymbol{F}_S^i + \boldsymbol{F}_T^i + \boldsymbol{F}_A^i \tag{1}$$

$$I^i \frac{\mathrm{d}\boldsymbol{W}^i}{\mathrm{d}t} + \boldsymbol{W}^i \times (I^i \boldsymbol{W}^i) = \boldsymbol{M}_S^i + \boldsymbol{M}_T^i + \boldsymbol{M}_A^i \tag{2}$$

where

$$I = \begin{bmatrix} I_{xx} & I_{xy} & I_{xz} \\ I_{xy} & I_{yy} & I_{yz} \\ I_{xz} & I_{yz} & I_{zz} \end{bmatrix} \tag{3}$$

Received July 12, 1991; revision received Oct. 15, 1993; accepted for publication Oct. 18, 1994.

*Manager, software system, Launch Vehicle Design Group.

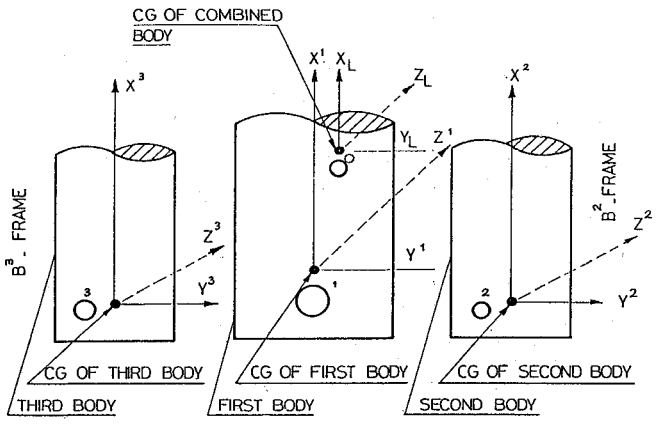

Fig. 1 Description of *L* frame and *B* frame and their transformations.

Since the body velocity and angular rates are same at the time of separation, we have at $t = 0$

$$W^i = W_0$$
$$V^i = W_0 \times d_0 \tag{4}$$

Kinetic Relations

With reference of the transformation from L frame to B frame, one can derive the following relationship[5] between the body angular rates W^i and the attitude angular rates as

$$\frac{d\phi^i}{dt} = W_x^i + \left(W_y^i \sin\phi^i + W_z^i \cos\phi^i\right)\tan\theta^i \tag{5}$$

$$\frac{d\theta^i}{dt} = W_y^i \cos\phi^i - W_z^i \sin\phi^i \tag{6}$$

$$\frac{d\psi^i}{dt} = \frac{W_y^i \sin\phi^i + W_z^i \cos\phi^i}{\cos\theta^i} \tag{7}$$

Since the body coordinate frame coincides with the L coordinate frame, we have at $t = 0$

$$\phi^i = \theta^i = \psi^i = 0 \tag{8}$$

Equations (1), (2), (5), (6), and (7) along with the boundary conditions [Eqs. (4) and (8)] will describe the motion of the bodies participating in the separation.

The occurrence of collisions[5] can be studied by selecting a suitable set of points on the separating bodies and computing the distances between them. The modeling of forces and moments acting on the separating bodies due to a separation system based on compressed springs and thrust has been investigated in detail in Ref. 6 and is not reproduced here.

Aerodynamic Characteristics of Separating Strap-on

As stated in the introduction, the aerodynamic characterization of a separated strap-on has been the most difficult task in the investigation of strap-on separation. With reference to the vehicle configuration shown in Fig. 2, the important aerodynamic forces and moments for separating strap-ons are the side forces, yawing moments, and axial forces. A discussion of the side force, axial force, and yawing moment for a small angle of incidence has been made in Ref. 1. For the purposes of strap-on separation, we need these aerodynamic coefficients for all possible orientations and gap distances. These data require a large number of wind-tunnel tests. In order to minimize (or avoid if possible) wind-tunnel testing, we tried to develop an aerodynamic model of separating strap-ons. In developing this model, we assume that the aerodynamic field is composed of interference aerodynamics and free-body aerodynamics. The free-body aerodynamics is due to strap-on geometry only. Since the Mach-number variations during the strap-on separation are negligible, the free-

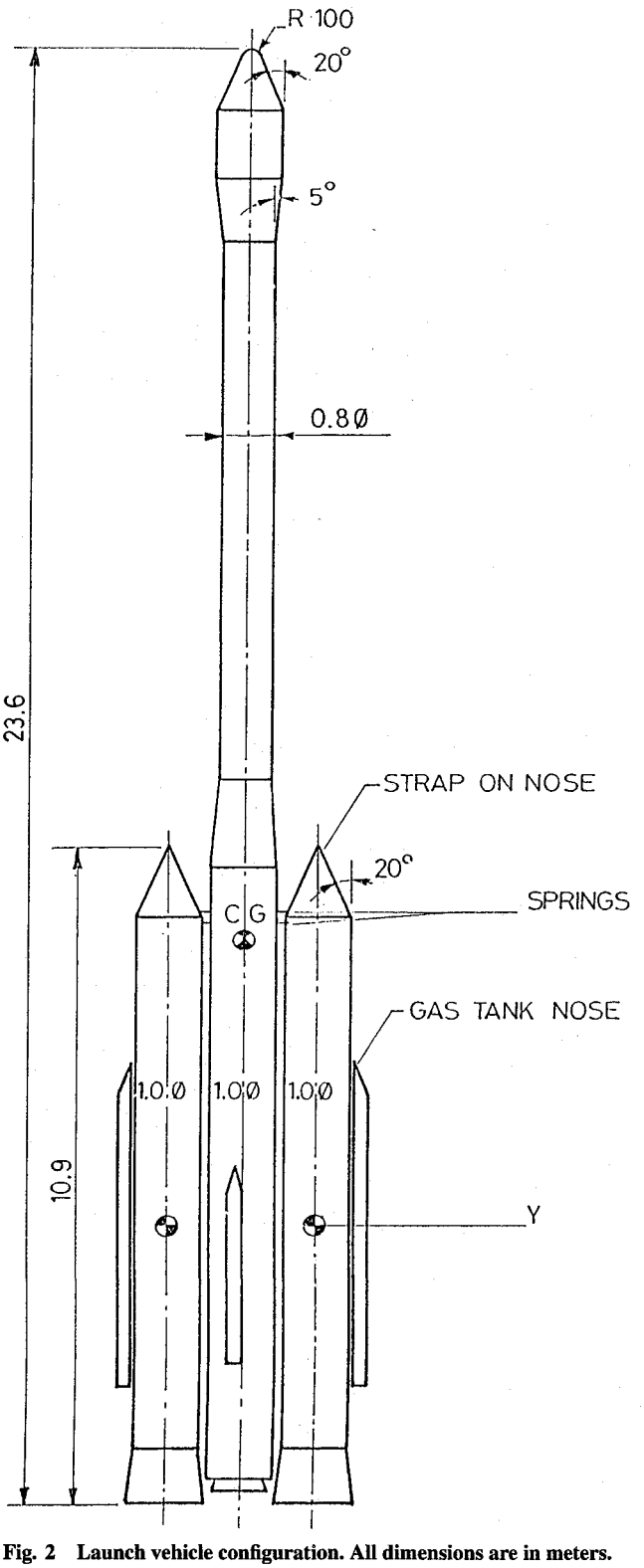

Fig. 2 Launch vehicle configuration. All dimensions are in meters.

Table 1 Aerodynamic coefficients of strap-on[a]

Quantity[b]	Sstrap-on booster	1.2-deg angle of incidence				4-deg angle of incidence			
		Leeward strap-on		Windward strap-on		Leeward strap-on		Windward strap-on	
CS	Top	0.24	0.27	0.25	0.25	0.26	0.26	0.20	0.18
	Bottom	0.27	0.31	0.23	0.24	0.26	0.29	0.25	0.26
	Average	0 .272		0.242		0.267		0.222	
CYM	Top	0.36	0.37	0.4	0.26	0.49	0.45	0.73	0.59
	Bottom	0.4	0.33	0.49	0.45	0.45	0.40	0.93	0.84
	Average	0.365		0.4		0.447		0.772	

[a]Just prior to separation: configuration of Fig. 2.
[b]Side force; acting away from core is positive. CYM: Yawing moment; nose opening moment is positive.

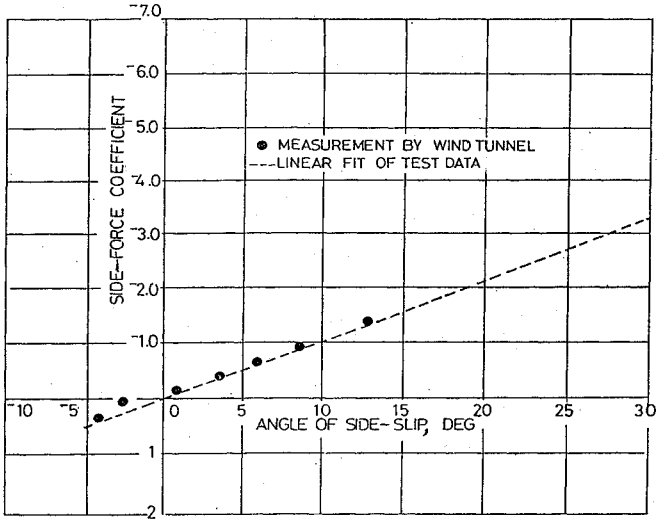

Fig. 3 Representation for free-body side-force coefficient.

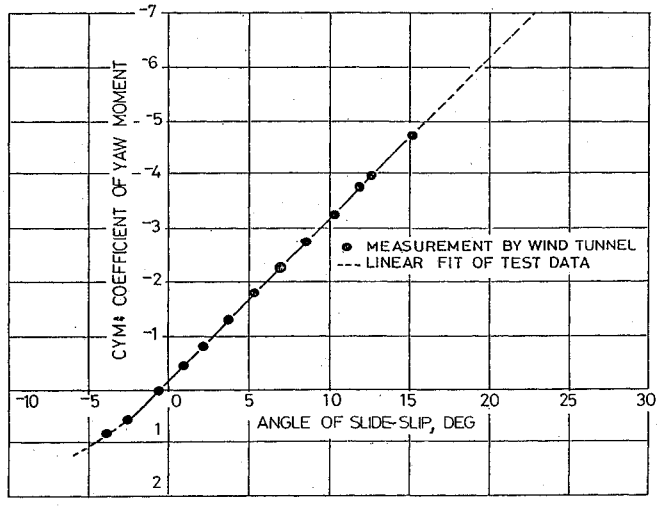

Fig. 4 Representation for free-body yawing-moment coefficient.

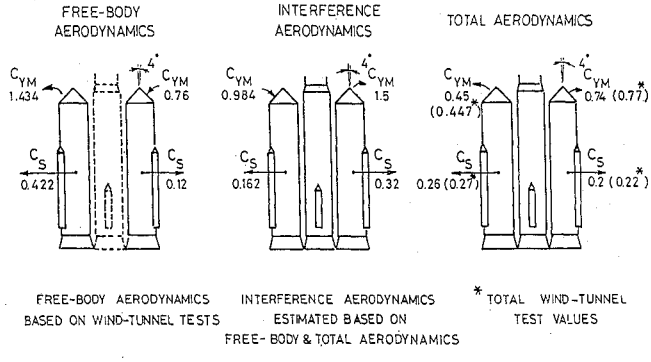

Fig. 5 Aerodynamic model for separation studies.

body aerodynamic field is dependent primarily on the sideslip angle of the strap-on. The sideslip angle of a strap-on is the angle between the core and the strap-on measured from the core vehicle towards the strap-on gas tank (positive anticlockwise). The interference aerodynamic field is due to the presence of the core in the vicinity of the strap-on. So the interference field depends on the body geometry of the strap-ons and core, the gap between strap-on and core, and the sideslip angle of the strap-on. Thus, the interference aerodynamic field is very complex and depends on a large number of parameters. During the initial phase of strap-on separation, the sideslip angles are small, and the interference field is primarily determined by the gap between strap-on and core. As the sideslip angle builds up, the gap between the core and strap-ons is increased and the role of the interference aerodynamic field is reduced. So we can represent the interference field by the gap distance between the core and the strap-on. It is assumed that this interference field decreases to zero at a distance of 2.5 diameters away from the core. Thus,

$$C_S(d, \beta) = C_{SF}(\beta) + C_{SI}(d) \tag{9}$$

$$C_{YM}(d, \beta) = C_{YMF}(\beta) + C_{SI}(d) \tag{10}$$

The axial-force coefficient primarily depends on the longitudinal gap and the sideslip angle. It has been observed that during the initial phase of strap-on separation, the variation of axial force with sideslip angle is not significant. Hence we have assumed that the axial force is solely dependent on longitudinal distance between strap-on and core.

Strap-on Separation Studies for an Initial 4-deg Angle of Incidence

As an illustration of the use of the aerodynamic model, we investigate the separation of the strap-on for the configuration shown in Fig. 2. Wind-tunnel tests were conducted[1] for the same configuration with an initial angle of incidence of 1.2 deg. We have studied the separation of the same strap-on for an initial angle of 4 deg. The resulting coefficients are presented in Table 1. The windward and leeward strap-ons have their gas-tank attachments in opposite directions (Fig. 2). So the separated strap-ons (without core) were tested in the same wind-tunnel for the leeward and the windward configuration at the same angle of incidence. The results of the wind-tunnel tests were fitted with linear functions of the sideslip angle. These are shown in Figs. 3 and 4. They represent the free-body aerodynamics of strap-ons for the present configuration. This linear fit allows us to extrapolate these aerodynamic coefficients beyond the wind-tunnel testing range (up to a sideslip angle of 12 deg).

For computing the aerodynamic interference field, the wind-tunnel test data on the side-force coefficient and yawing-moment coefficient for initial angle of incidence 1.2 deg were used (Table 1). Using these data and the free-body aerodynamics for a 1.2-deg initial angle of incidence, the aerodynamic interference field for this

Table 2 Strap-on separation environment

Strap-on separation altitude	14 km
Dynamic pressure	30 kPa
Angle of attack	4 deg
Mach no.	2.1
Strap-on tail-off thrust (vac)	2.5 kN
Core-vehicle thrust (vac) at separation	364 kN
Springs	
No. of springs to each strap-on	4
Spring stiffness for each of two lower springs	788 kN/m
Spring stiffness for each of two upper springs	516 kN/m
Spring compression (same for all springs)	90 mm
Force and moments due to tail-off thrust	
Axial force	2.7 kN
Side force	−0.391 kN
Yawing moment	1.329 kN/m

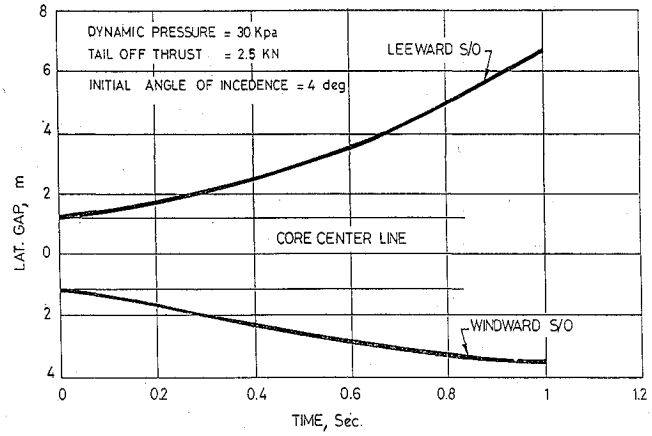

Fig. 6 Predicted lateral-gap buildup history.

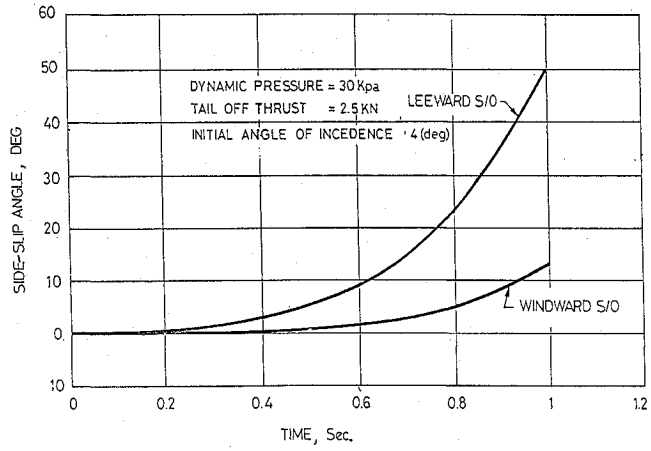

Fig. 7 Predicted sideslip-angle development history.

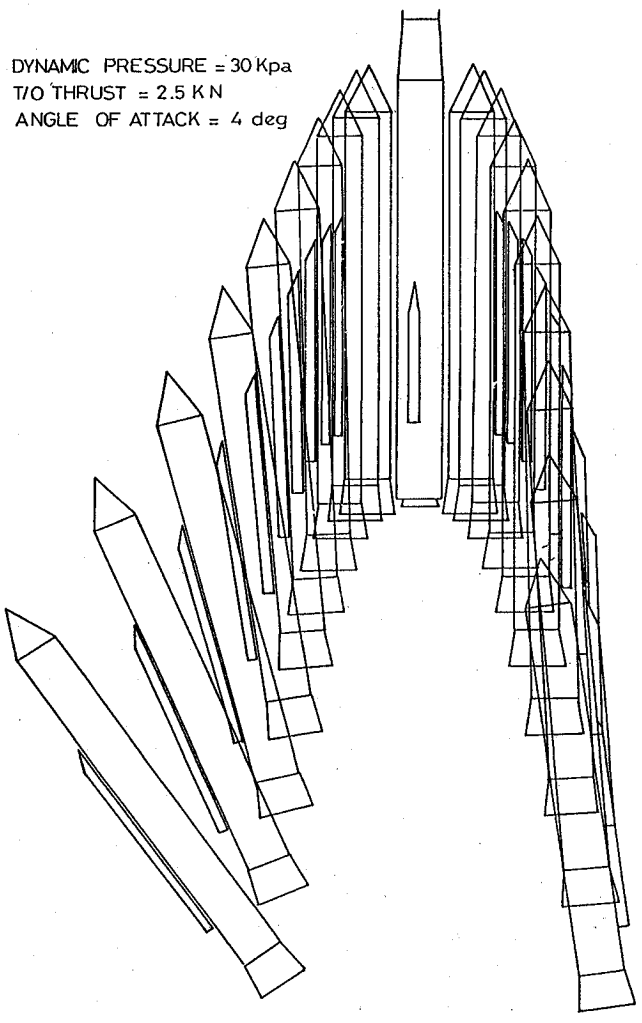

Fig. 8 Trace of separating strap-ons.

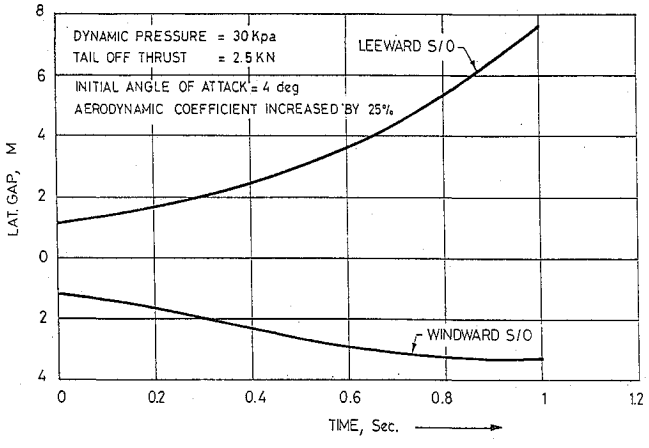

Fig. 9 Predicted lateral-gap buildup history (25% increase of aerodynamics).

configuration has been generated for zero gap using the Eqs. (9) and (10). Along with this interference field, the free-body aerodynamic coefficients for an initial angle of incidence of 4 deg and zero gap are given in Fig. 5. The complete aerodynamic coefficients for this configuration at a 4-deg initial angle of incidence and zero gap are also shown in the same figure. One can compare these aerodynamic coefficients with those due to wind-tunnel test values. Other parameters pertinent to this configuration are presented in Table 2.

The development of the side gap and the sideslip angle for a leeward and a windward strap-on is shown in Figs. 6 and 7. One can observe that the side-gap development for windward strap-on is slow. The traces of separating strap-ons are shown in Fig. 8. One can find from this figure that the separation of a strap-on is collision-free. In order to build robustness into the separation, we increase the aerodynamic coefficient by 25% in the worse combinations and reinvestigate the strap-on separation. A worse combination corresponds to a reduction of the aerodynamic coefficient if it is favorable to safe separation, and to an increase in the aerodynamic coefficient if it is adverse to safe separation. For example, the free-body side-force coefficient for the leeward strap-on is favorable to separation, so it is reduced, while the coefficient for the windward strap-on is adverse, so it is increased. The time history of side-gap, sideslip angle, and traces of the separating strap-ons is shown in Figs. 9, 10,

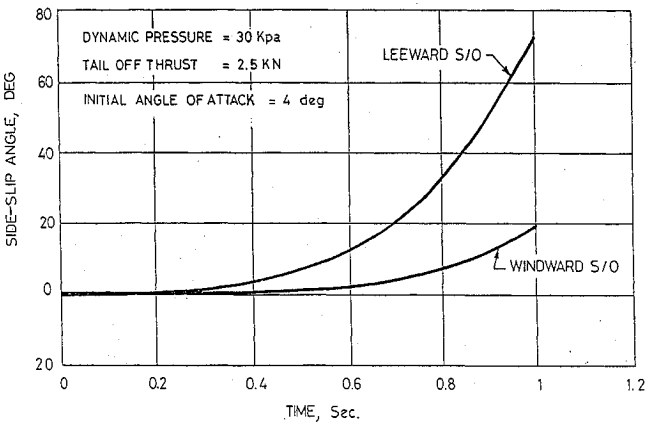

Fig. 10 Predicted sideslip-angle development history (25% increase of aerodynamics).

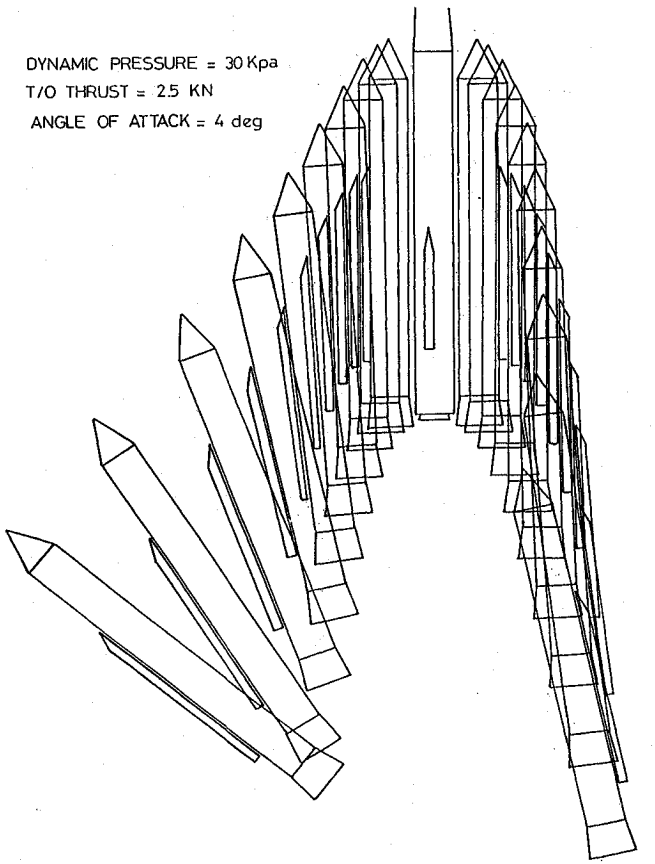

Fig. 11 Trace of separating strap-ons for 25% increase of aerodynamics.

and 11, respectively. One can conclude from a comparison of the results in Figs. 6 and 9 that the lateral gap development is slowed down for a windward strap-on when the aerodynamic field is increased by 25%. The separation is still collision-free.

Conclusions

In this paper, an attempt has been made to develop an empirical aerodynamic model for strap-on separation studies. In this model, the complex aerodynamic field is assumed to be made up of free-body aerodynamics and interference aerodynamics. The free-body aerodynamic field is assumed to be dependent only on the sideslip angle. The interference aerodynamic field is dependent on the gap distance of the strap-on and the core vehicle. The free-body aerodynamic field of a strap-on can be generated analytically or experimentally. Once the freebody aerodynamic field is known, the interference aerodynamic field can be estimated by using very limited wind-tunnel tests conducted for strap-on aerodynamics at the same prescribed initial angle of incidence for the zero gap. Using the above concept, the complete aerodynamic field needed for strap-on separation studies can be generated. Thus, the present method has very few wind-tunnel test requirements.

Using this model and the wind-tunnel test data for an initial angle of incidence of 1.2 deg, the complex aerodynamic field for strap-on separation studies at an initial angle of incidence of 4 deg was modeled, and separation studies were conducted. Collision-free separation was predicted even with 25% adverse aerodynamics. This aerodynamic model is therefore very handy for various investigations related to strap-on separation.

Acknowledgments

The authors wish to record their deep sense of gratitude to S. Srinivasan, PD, ILVP, VSSC, for his constant encouragement for these studies. They are also thankful to N. Sundararajan, former Group Director, LVDG, VSSC, and Shri. E. Janardhana, Group Head, LVDG, VSSC, for their valuable suggestions.

References

[1]Sundaramoorthy, H., Narayana, K. Y., Suryanarayana, G. K., Lochan, R., and Nair, K. G. S., "Wind Tunnel Investigations of Strap-on Booster Separation Characteristics of Launch Vehicle," *Journal of Aeronautical Society of India*, Vol. 38, No. 4, Nov. 1986, pp. 215–220.

[2]Decker, J. P., "Experimental Aerodynamic Analysis of Stage Separation of Reusable Launch Vehicle," NASA SP-148, May 1967.

[3]Decker, J. P., and Joseph, G., "An Exploratory Study of Parallel Stage Separation of Reusable Launch Vehicles," NASA-TND-4565, Oct. 1968.

[4]Biswas, K. K., and Krishnan, C. G., "On Dynamics of Separating Strapons for Reallocated TVC-Tank Configuration of ASLV-D3," Indian Space Research Organisation, VSSC-ILVP-LVDG-TN-006/89, June 1989.

[5]Biswas, K. K., and Alex, L., "Dynamics of Heat Shield Jettisoning System," National Seminar on Aerospace Related Mechanism, Indian Space Research Organisation, VSSC Number, Aug. 1985, pp. LV3.1–LV3.28.

[6]Biswas, K. K., Alex, L., Lochan, R., and Nair, K. G. S., "SEP6DT-6D Trajectory Simulation Package for Separation Studies of Multistage Launch Vehicle," Indian Space Research Organisation, VSSC-TR-O14-84, June 1984.